

Supplementary Information

Surface Acoustic Wave-Assisted Swing-Angle Spray: From Mechanism Investigation to Deposition Characteristics and In Vivo Wound Healing

Chenhui Gai^a, Yu Gu^a, Qutong Yang^b, Suxiao Zhao^a, Yizhan Ding^a, Yulin Lei^a,

Junlong Han^{c,*}, Hong Hu^{a,*}, Chen Fu^{b,*}

*a School of Mechanical Engineering and Automation, Harbin Institute of Technology,
Shenzhen, 518055, China*

*b College of Physics and Optoelectronic Engineering, Shenzhen University, Shenzhen,
518060, China*

*c School of Automotive & Transportation Engineering, Shenzhen Polytechnic
University, Shenzhen, 518055, China*

* Corresponding author

Email address: hanjunlong@szpu.edu.cn (Junlong Han), honghu@hit.edu.cn (Hong Hu), chenfu@szu.edu.cn (Chen Fu)

The file includes:

Fig. S1 to S7

Table. S1

Video S1 to S2

Data S1

Supplementary figure, video and data captions

Fig. S1. The experimental setup of the SAW-SAS.

Fig. S2. Laser Doppler Vibrometer (LDV) measurement system.

Fig. S3. Frequency Response (S11) Spectrum of the SAW Device.

Fig. S4. Image processing of spray deposition characteristics.

Fig. S5. Spray deposition on water-sensitive paper when swing-angle at approximately 5° .

Fig. S6. Spray deposition on water-sensitive paper when swing-angle at approximately 30° .

Fig. S7. Spray deposition on water-sensitive paper when swing-angle at approximately 45° .

Table. S1. The standard deviation for all key parameters in Fig. 4(a)

Video S1 Small swing-angle spray.

Video S2 Large swing-angle spray.

Data S1 SAW-SAS Deposition Characteristics.

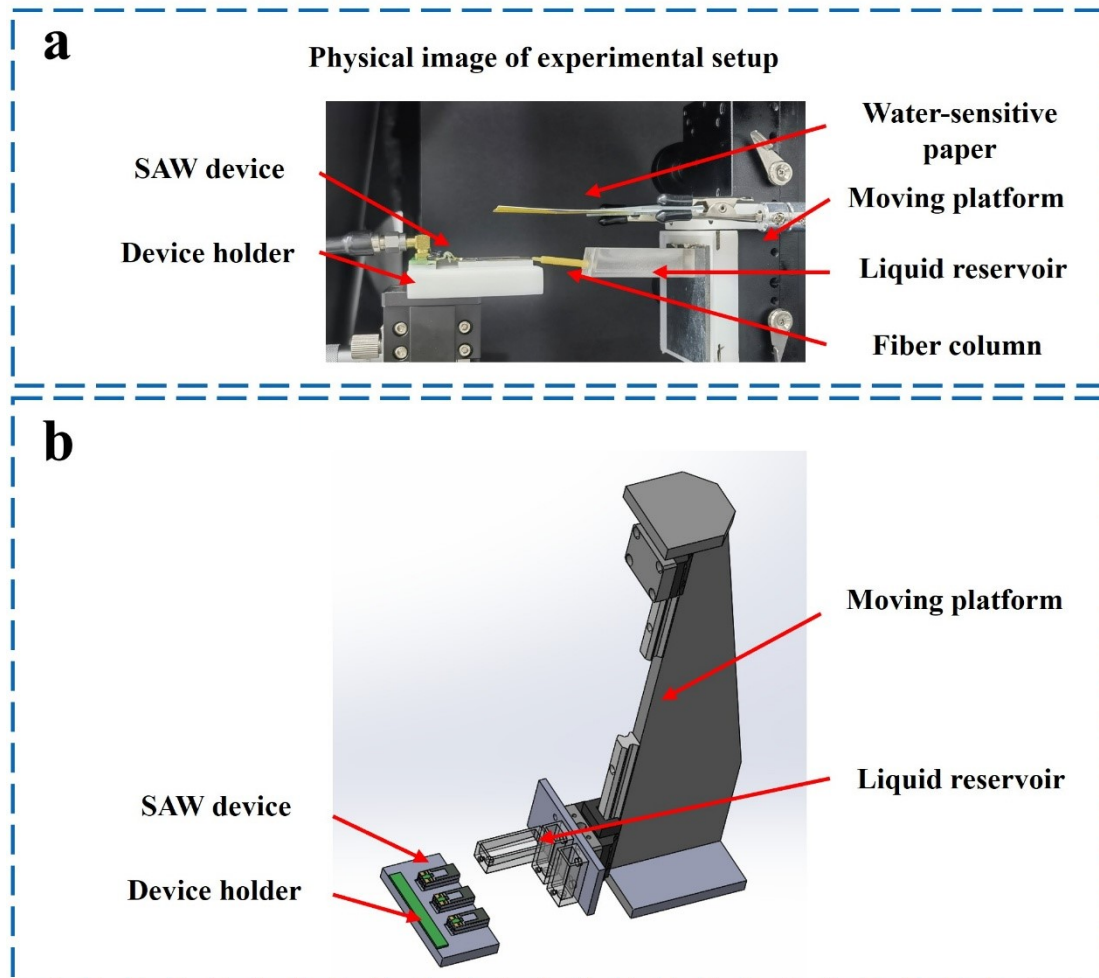


Fig. S1. The experimental setup of the SAW-SAS. (a) Physical image of experimental setup. (b) Schematic diagram of experimental setup.

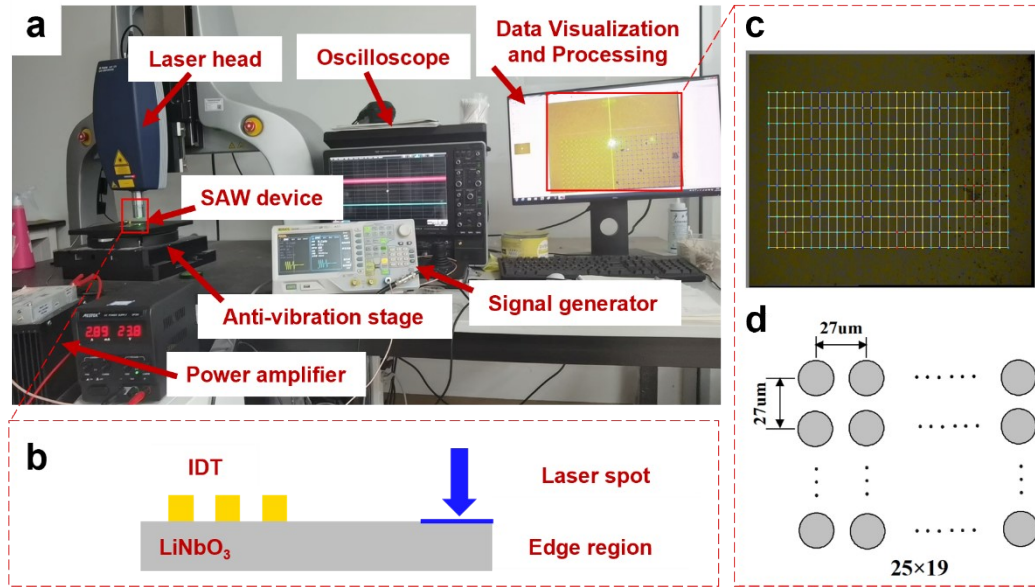


Fig. S2. Laser Doppler Vibrometer (LDV) measurement system. (a) Photograph of the experimental setup, integrating a SAW excitation module and a laser-based detection and analysis module. (b) Schematic illustrating the laser spot precisely focused on the device's edge region. (c) Micrograph of the device edge showing the $650 \mu\text{m} \times 500 \mu\text{m}$ scanned grid. (d) Schematic of the 25×19 scan point array with $27 \mu\text{m}$ spacing.

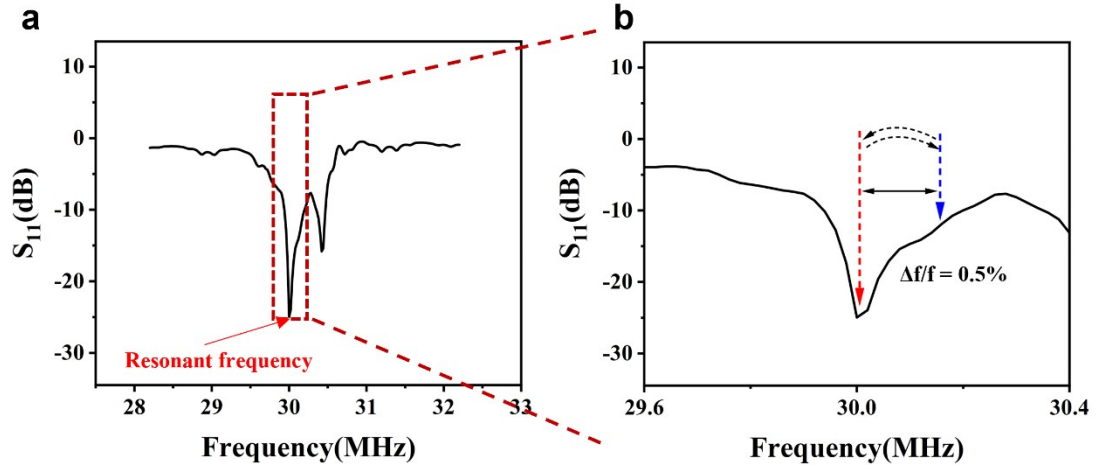


Fig. S3. Frequency Response (S₁₁) Spectrum of the SAW Device. (a) S₁₁ (return loss) measurement showing a clear resonant frequency at approximately 30.0 MHz. (b) Magnified view of the resonant peak, illustrating the 0.5% relative frequency deviation range on the high-frequency (right) side of the peak, which is used for the SAW-SAS swing-angle modulation. The non-linear slope of this curve explains the non-uniform angle-to-frequency response shown in **Fig. 3(b)**.

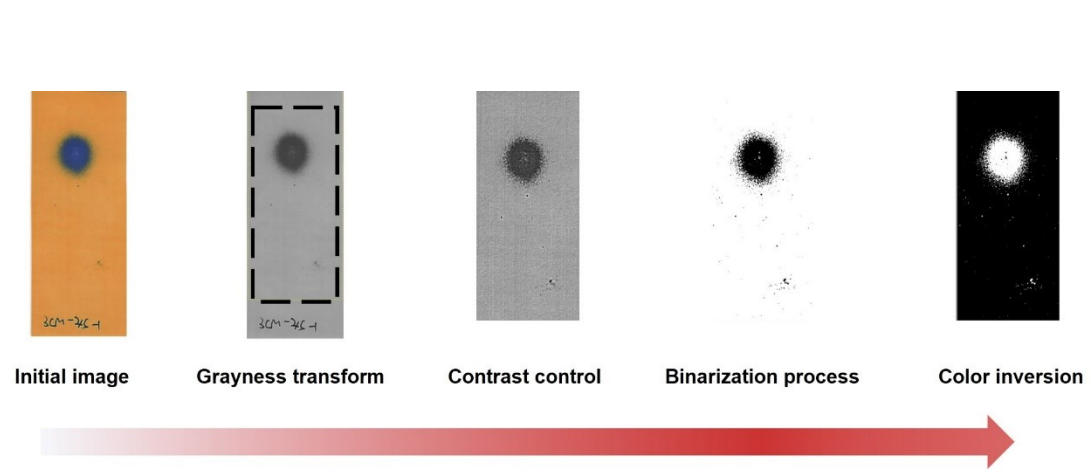


Fig. S4. Image processing of spray deposition characteristics.

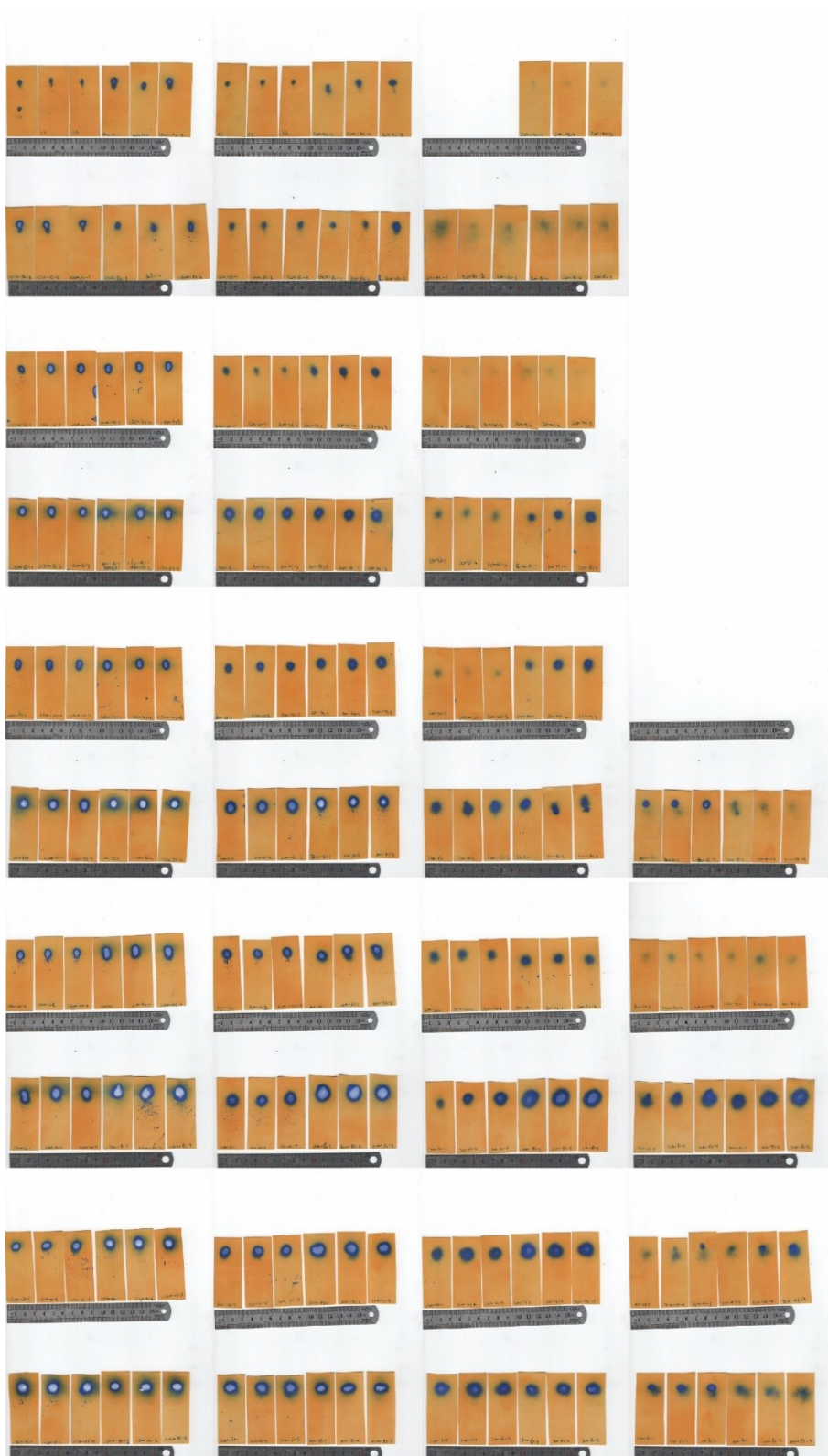


Fig. S5. Spray deposition on water-sensitive paper when swing-angle at approximately 5°.

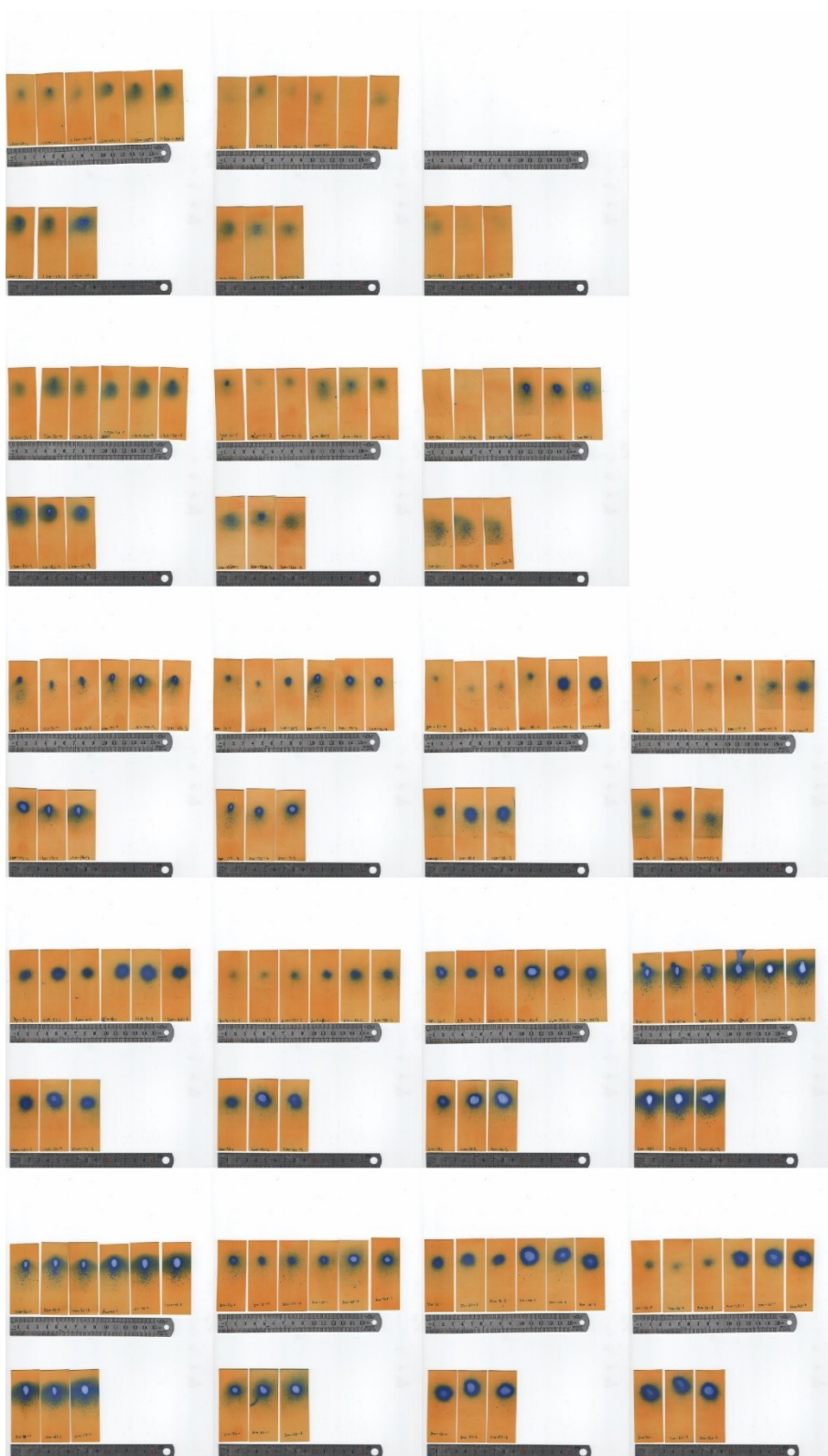


Fig. S6. Spray deposition on water-sensitive paper when swing-angle at approximately 30°.

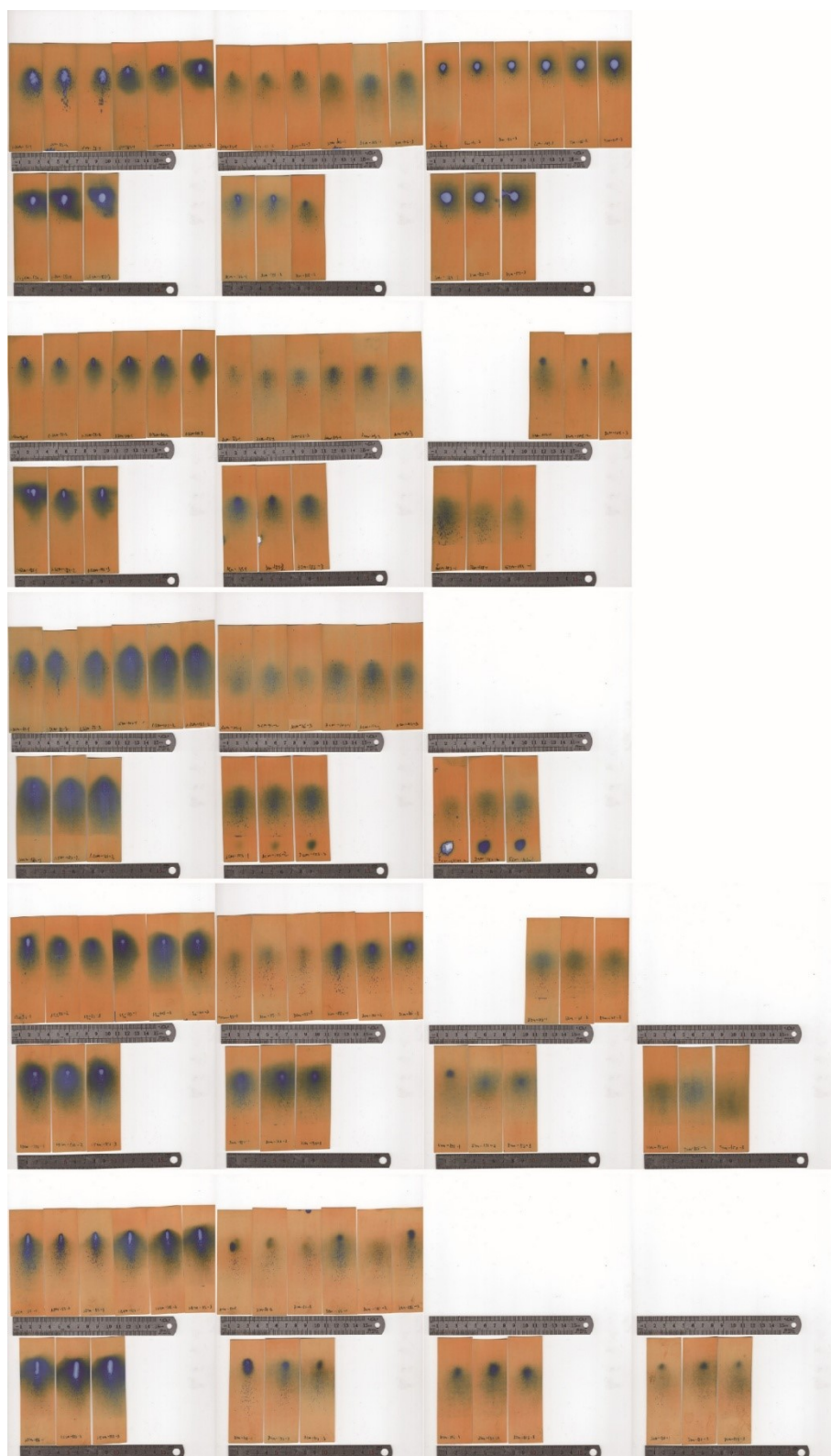


Fig. S7. Spray deposition on water-sensitive paper when swing-angle at approximately 45°.

Table. S1. The standard deviation for all key parameters in **Fig. 4(a)**

Propagation	DV1	SD	VMD	SD	DV9	SD	NMD	SD	Coverage	SD
Angle (°)	(μm)	(μm)	(μm)	(μm)	(μm)	(μm)	(μm)	(μm)	(%)	(%)
5	72.85	0.73	114.05	2.40	2389.12	214.93	119.52	5.63	5.39	1.05
	73.13	2.05	109.86	6.57	3438.67	1246.10	119.18	8.92	9.69	3.82
	73.94	1.37	119.13	3.72	3944.28	624.35	128.81	7.31	12.58	4.01
	74.36	3.91	125.26	14.85	4453.49	361.93	130.09	14.15	16.53	2.49
	74.36	3.06	116.58	12.71	4904.94	509.03	124.07	13.96	20.00	3.85
	74.82	2.83	107.95	9.38	1499.13	146.27	111.50	13.02	6.97	2.71
30	74.89	1.39	115.75	3.02	2812.74	547.96	119.76	6.58	13.95	3.81
	74.52	1.96	121.26	9.14	2987.24	732.77	123.50	8.17	11.98	2.19
	74.54	3.40	117.58	21.05	2223.81	873.44	120.82	17.62	15.47	11.06
	77.32	3.05	126.48	17.78	3554.51	415.60	129.21	15.19	30.57	3.15
	77.65	1.23	122.03	5.75	2319.87	298.81	124.72	3.16	14.95	6.42
	77.97	1.67	121.73	7.64	501.59	599.58	123.91	3.88	16.43	4.78
45	80.90	0.41	143.58	6.67	3236.15	192.97	137.84	5.39	22.53	4.26
	80.85	1.29	148.82	9.82	3391.67	223.41	141.25	6.53	25.54	6.91
	78.64	0.73	138.60	5.27	286.53	180.33	128.98	2.40	10.08	7.06